Journal of Developmental Origins of Health and Disease (2017), **8**(6), 665–673.

doi:10.1017/S2040174417000484

ORIGINAL ARTICLE

Intrauterine growth restriction-induced deleterious adaptations in endothelial progenitor cells: possible mechanism to impair endothelial function

V. Oliveira[1], L. V. de Souza[1], T. Fernandes[2], S. D. S. Junior[3], M. H. C. de Carvalho[4], E. H. Akamine[4], L. C. Michelini[3], E. M. de Oliveira[2] and M. d. C. Franco[1]*

[1]*Nephrology Division, School of Medicine, Federal University of São Paulo, São Paulo, Brazil*
[2]*School of Physical Education and Sport, Biochemistry and Molecular Biology Laboratory, University of São Paulo, São Paulo, Brazil*
[3]*Physiology Department, Institute of Biomedical Sciences, University of São Paulo, São Paulo, Brazil*
[4]*Pharmacology Department, Institute of Biomedical Sciences, University of São Paulo, São Paulo, Brazil*

Intrauterine growth restriction (IUGR) can induce deleterious changes in the modulatory ability of the vascular endothelium, contributing to an increased risk of developing cardiovascular diseases in the long term. However, the mechanisms involved are not fully understood. Emerging evidence has suggested the potential role of endothelial progenitor cells (EPCs) in vascular health and repair. Therefore, we aimed to evaluate the effects of IUGR on vascular reactivity and EPCs derived from the peripheral blood (PB) and bone marrow (BM) *in vitro*. Pregnant Wistar rats were fed an *ad libitum* diet (control group) or 50% of the *ad libitum* diet (restricted group) throughout gestation. We determined vascular reactivity, nitric oxide (NO) concentration, and endothelial nitric oxide synthase (eNOS) protein expression by evaluating the thoracic aorta of adult male offspring from both groups (aged: 19–20 weeks). Moreover, the amount, functional capacity, and senescence of EPCs were assessed *in vitro*. Our results indicated that IUGR reduced vasodilation via acetylcholine in aorta rings, decreased NO levels, and increased eNOS phosphorylation at Thr495. The amount of EPCs was similar between both groups; however, IUGR decreased the functional capacity of EPCs from the PB and BM. Furthermore, the senescence process was accelerated in BM-derived EPCs from IUGR rats. In summary, our findings demonstrated the deleterious changes in EPCs from IUGR rats, such as reduced EPC function and accelerated senescence *in vitro*. These findings may contribute towards elucidating the possible mechanisms involved in endothelial dysfunction induced by fetal programming.

Received 18 October 2016; Revised 26 May 2017; Accepted 30 May 2017; First published online 10 July 2017

Key words: endothelial dysfunction, endothelial progenitor cells, intrauterine growth restriction, nitric oxide

Introduction

Clinical and experimental data have revealed deleterious adaptations in the vasculature as a hallmark of the fetal programming process.[1–11] These responses are attributed to insults (e.g. maternal diet manipulation, hypoxia, and uteroplacental insufficiency) that occur during the critical window of fetal development.[5–12] Indeed, intrauterine growth restriction (IUGR) is associated with abnormalities in the modulatory ability of the vascular endothelium, resulting in reduced endothelium-dependent relaxation.[7–9] Several mechanisms are involved in vascular programming; increased reactive oxygen species (ROS) levels and reduced antioxidant capacity have been observed in IUGR animals.[8–10,13] In addition, decreased endothelial nitric oxide synthase (eNOS) messenger RNA expression, methylation of the NOS3 promoter, and lower nitric oxide synthase (NOS) activity can contribute to NO reduction in different vascular beds.[4,14] Together, these adaptations may lead to an increase in cardiovascular events in adult life.

*Address for correspondence: M. d. C. Franco, Division of Nephrology School of Medicine, Federal University of São Paulo, Rua Botucatu 703, SP 04023-062, Brazil
(Email: maria.franco@unifesp.br)

Asahara *et al.* have isolated and characterized putative endothelial progenitor cells (EPCs) from the peripheral blood (PB) to investigate their possible roles.[15] EPCs are a heterogeneous population of cells in different states of maturation derived from the bone marrow (BM).[16,17] These cells exhibit the capacity to proliferate and migrate to injured sites where they play a role in several physiological repair processes such as reendothelization and vascular integrity maintenance.[18–20] Indeed, EPCs can differentiate into mature endothelial cells or activate resident endothelial cells by releasing paracrine factors.[21] Cardiovascular risk factors can reduce both EPC number and functions.[21,22] Furthermore, the properties of EPCs can be impaired under pathological conditions such as hypertension, vascular dysfunction, and heart failure, thus contributing to the prognosis of cardiovascular diseases.[23–26]

It is known that IUGR could induce harmful changes in EPCs.[27] Ligi *et al.* have extracted EPCs from the umbilical cord of newborns with IUGR and found a significant reduction in functional capacity, evidenced by the lower number of colony-forming units (CFUs) and the longer time in establishing colonies *in vitro*.[27] In addition, the angiogenic capacity of EPCs was reduced, and senescence was enhanced.[27] Therefore, IUGR may be an additional risk factor for EPC dysfunction.

Given that EPC dysfunction is also present in cases of altered flow-mediated vasodilation,[28–30] we hypothesized that EPC functional impairment could be a possible link between IUGR and reduced endothelium-dependent vasodilation in rats. Therefore, this study investigated the possible effects of IUGR on the vascular reactivity, EPC number, and EPC function of adult male rat offspring *in vitro*.

Materials and methods

All procedures were approved by the Ethical Committee for Animal Research (Protocol Number: 836.880) at the Federal University of São Paulo and were in accordance with the guidelines for ethical conduct in the care and use of animals proposed by the Brazilian Society of Laboratory Animal Science (SBCAL/COBEA).

Adult male and female Wistar rats purchased from the Institute of Biomedical Sciences of the University of São Paulo were kept at a controlled room temperature in a light–dark cycle (12:12 h) with free access to standard rat chow and tap water. As previously described, female Wistar rats were mated with male Wistar rats (age range: 14–16 weeks) overnight. The presence of spermatozoa in the vaginal smear was considered as the day of conception (day 0). Each pregnant rat was individually housed in standard cages and randomly divided into one of two groups: the control group (CT, $n = 10$), which were fed a standard laboratory animal diet (Nuvilab CR1; based on the recommendation of the National Research Council and National Institutes of Health, USA) *ad libitum*, and the restricted group (RT, $n = 11$), which were fed 50% of the typical daily food intake (determined by the amount of food consumed by the CT group during the gestation period). The pups were weighed immediately after they were born, and the mothers from the RT group were fed an *ad libitum* diet. At birth, litter size was standardized to eight pups (four males and four females) for both groups to prevent alterations in neonatal growth due to decreased milk availability during suckling. The offspring were nursed by their mothers until weaning at day 21. The present study was conducted only on male offspring (age range: 19–20 weeks). To avoid litter effects, two animals from each litter were chosen for each experiment. Female offspring were euthanized (age range: 14–16 weeks) for use in another study unrelated to the present research.

Resting arterial blood pressure evaluation

Resting systolic blood pressure was noninvasively determined using a computerized tail-cuff system (PowerLab 4/S; ADInstruments Pty Ltd., Castle Hill, Australia). Rats were acclimatized to the apparatus in daily sessions over 5 days (1 week before measurements).

Assessment of vascular reactivity in vitro

Under anaesthesia (50 mg/kg sodium thiopental, administered intraperitoneally), the thoracic aorta was quickly harvested and cleaned to remove connective tissues in cold Krebs–Henseleit solution (118 mM NaCl, 4.7 mM KCl, 25 mM $NaHCO_3$, 2.5 mM $CaCl_2{\cdot}2H_2O$, 1.2 mM KH_2PO_4, 1.2 mM $MgSO_4{\cdot}7H_2O$, 11 mM glucose, and 0.01 mM EDTA; pH 7.4). Two segments of the thoracic aorta from each animal (4 mm in length) were mounted in an isolated chamber containing Krebs–Henseleit solution, gassed with 95% O_2 and 5% CO_2, and maintained at 37°C. A basal tension of 1.5 g was applied to each segment of the thoracic aorta. Isometric tension was recorded using an isometric force transducer (TRI 210; Letica, Barcelona, Spain) connected to an acquisition system (PowerLab 8/30; ADInstruments Pty Ltd.). The preparations were equilibrated for 1 h (the Krebs–Henseleit solution was changed every 20 min), followed by tension adjustments. After equilibration, the cumulative concentration-response curves to the agonists acetylcholine (ACh: 10^{-9}–10^{-5} M) and sodium nitroprusside (SNP: 10^{-9}–10^{-5} M) were obtained in pre-contracted (noradrenaline: 10^{-7} M) endothelium-intact aorta rings. Arterial integrity was assessed by stimulation of the vessels with potassium chloride (KCl: 120 mM). Endothelial integrity was assessed by evaluating the relaxant effect of ACh (10^{-6} M) in vessels pre-contracted with noradrenaline (10^{-7} M). The agonist concentration-response curves were fitted using a nonlinear interactive fitting software (GraphPad Prism 5.0; GraphPad Software Inc., USA). The maximal response (E_{max}) and potency ($-\text{LogEC}_{50}$) are expressed as mean ± S.E.M. and a confidence interval, respectively.

Thoracic aorta preparation for NO and Western blotting assays

Under anaesthesia (50 mg/kg sodium thiopental, administered intraperitoneally), the thoracic aorta was quickly harvested and cleaned to remove connective tissues in cold Krebs–Henseleit solution. Then, it was immediately frozen and stored at −80°C. The tissues were prepared using lysis buffer (100 mM Tris-HCl at pH 7.4, 100 mM sodium pyrophosphate, 10 mM sodium orthovanadate, 100 mM NaF, 10 mM EDTA, 2 mM phenylmethylsulfonyl fluoride, 0.01 mg/ml aprotinin, and 1% Triton X-100) and centrifuged (15,000 ***g***, 30 min, 4°C), and the supernatant was collected. The protein content of the lysates was determined using Pierce BCA (bicinchoninic acid) Protein Assay Kit (Pierce Biotechnology, Rockford, IL, USA).

NO measurement

NO is extremely unstable; thus, the nitrite and nitrate in thoracic aorta homogenates were re-converted to NO via reaction with vanadium. NO was measured by the chemiluminescence method using a NO analyser (Sievers Instruments Inc., Boulder, CO, USA), which is based on the gas-phase chemiluminescence reaction between NO and ozone. The results were analysed by software, and the concentration of each sample was normalized to their respective protein concentrations.[31]

https://doi.org/10.1017/S2040174417000484 Published online by Cambridge University Press

Western blotting analysis

The supernatant from thoracic aorta homogenates (70 μg) was treated with Laemmli buffer containing 200 mmol/l dithiothreitol and subjected to sodium dodecyl sulfate polyacrylamide gel electrophoresis with 7.5% polyacrylamide gels. Following electrophoresis, proteins were electro-transferred overnight onto nitrocellulose membranes (BioRad, Hercules, CA, USA). After blocking nonspecific sites with T-TBS buffer containing 3% bovine serum albumin at room temperature for 2 h, the membranes were incubated overnight at 4°C with the primary antibody anti-p-eNOS^{Ser1177} (1 : 1000; Cell Signaling, USA), anti-p-eNOS^{Thr495} (1:1000; Millipore, USA), or anti-t-eNOS (1 : 1000; Cell Signaling). The primary antibodies were detected using peroxidase-conjugated secondary anti-rabbit IgG (1:1500; Jacskon ImmunoResearch Inc., West Grove, PA, USA) and anti-mouse IgG (1:10000; Jackson ImmunoResearch Inc.) antibodies. The immune complexes were detected using an enhanced luminol chemiluminescence system (ECL Plus; GE Healthcare, Little Chalfont, UK) and subsequently photographed (Gel Logic 2200 Pro; Nova Analítica, Brazil). The bands were analysed using ImageJ software (National Institutes of Health, Bethesda, MD, USA). t-NOS was expressed as the ratio between its mean optical density and the optical density of Ponceau staining.[32,33] The expression of p-eNOS^{Ser1177} and p-eNOS^{Thr495} was normalized to that of t-eNOS. The results are expressed as the optical density ratio of p-eNOS^{Ser1177} and p-eNOS^{Thr495} to t-eNOS.

Isolation of PB and BM mononuclear cells

Under anaesthesia (50 mg/kg sodium thiopental, administered intraperitoneally), 5–6 ml of PB was collected from the abdominal aorta in ethylenediaminetetraacetic acid (EDTA) tubes, and both tibias and femurs were obtained and placed in sterile phosphate-buffered saline (PBS) solution containing penicillin–streptomycin (100 μl/l; Sigma-Aldrich Co., USA). Under sterile conditions, tibia and femur cavities were flushed with Dulbecco's modified Eagle's medium (DMEM; GIBCO, USA) to obtain the BM. Both the PB and BM were fractionated by density gradient centrifugation (2500 rpm, 25 min, 20–22°C) (Ficoll-Paque; GE Healthcare, Munich, Germany). Then, monoculear cells (MNCs) obtained from the samples were quantified, and their *in vitro* function and senescence were evaluated.[34]

EPC immunophenotyping and quantification by flow cytometry

The MNCs derived from the PB and BM were considered as EPCs ($CD34^+/VEGFR2^+$ cells). Briefly, 1×10^6 MNCs were individually incubated at room temperature in the dark for 30 min with the antibodies anti-CD34-PE-Cy7 (Bioss, Woburn, MA, USA) and VEGFR2-FITC (Bioss) or the isotype controls anti-IgG-PE-Cy7 (BioLegend, San Diego, CA, USA) and IgG-FITC (BioLegend). The negative control was also incubated at room temperature in the dark for 30 min. After incubation, the cells were washed with PBS and fixed in 1% paraformaldehyde solution. Fixed cells were stored at 4°C in the dark for 15–20 h and evaluated using a flow cytometer (FACSCanto; BD Biosciences, USA) by collecting 1,000,000 events. The data were analysed using BD FACSDiva software (BD Biosciences). Gates were established on the forward-scatter and side-scatter (FSC/SSC) plots corresponding to selected MNCs, followed by CD34-PE-Cy7 and VEGFR2-FITC (Supplementary material Figure). The number of EPCs ($CD34^+/VEGFR2^+$) was calculated as the percentage of MNC events.[34]

Assay of EPC functional capacity in vitro

The CFUs of MNCs from the PB and BM were evaluated *in vitro*. Briefly, 5×10^6 MNCs were cultured (37°C, 5% CO_2, 95% humidity) on six-well plates pre-coated with fibronectin (BioCoat; BD Biosciences), seeded with EndoCult medium (STEMCELL Technologies, Vancouver, Canada). After 48 h, 1×10^6 non-adherent cells were transferred in triplicate to 24-well plates pre-coated with fibronectin and cultured for 72–96 h (37°C, 5% CO_2, 95% humidity) in EndoCult medium. Subsequently, the CFUs were manually counted by two blinded observers using an inverted microscope (Nikon Instruments Inc., USA).[34]

Assay of EPC senescence in vitro

Initially, 5×10^6 MNCs from the BM were cultured (37°C, 5% CO_2, 95% humidity) on six-well plates pre-coated with fibronectin (BioCoat), seeded with EndoCult medium (STEMCELL Technologies). After 48 h, 1×10^6 non-adherent cells were washed twice with PBS and fixed in 2% paraformaldehyde at room temperature for 3 min. Then, the cells were washed with PBS and incubated in duplicate (37°C, 5% CO_2, 95% humidity) for 24 h in β-galactosidase solution with EGM-2 medium (Lonza Group Ltd., Basel, Switzerland). Cells positive for SA-β-Gal exhibited a blue phenotype and were considered as senescent cells, and they were manually counted by two-blinded observers using an inverted microscope (Nikon Instruments Inc., USA).[34]

Statistical analysis

Statistical analysis was performed using GraphPad Prism 5.0 (GraphPad Software Inc., USA). Results are expressed as mean ± S.E.M. The data were analysed by an independent Student's *t*-test, and the significance level was set at $P < 0.05$.

Results

At birth, the body weight of pups in the RT group was significantly reduced compared with that of pups in the CT group (CT: 6.6 ± 0.11 g *v.* RT: 4.5 ± 0.14 g; $n = 16$; $P = 0.001$). However, between 19 and 20 weeks of age, both groups exhibited similar body weights (CT: 398.40 ± 11.24 g *v.* RT: 396.1 g ± 18.82 g; $n = 16$; $P = 0.787$). Blood pressure levels were significantly

https://doi.org/10.1017/S2040174417000484 Published online by Cambridge University Press

higher in RT offspring than in CT offspring (CT: 110 ± 3 mmHg *v.* RT: 123 ± 2 mmHg; $n = 7$; $P = 0.004$).

IUGR-induced reduction in endothelium-dependent relaxation in thoracic aorta rings

The endothelium-dependent vasodilator ACh induced a concentration-dependent relaxation in noradrenaline-pre-contracted thoracic aorta rings from RT and CT offspring. On the other hand, we found that the maximal vasodilation response to ACh was significantly reduced in the RT group when compared with that in the CT group (CT: 90.2 ± 1.7% *v.* RT: 65.0 ± 4.4%; $n = 8$; $P = 0.001$) (Fig. 2a). The NO donor SNP also promoted a concentration-dependent vasodilation in noradrenaline-pre-contracted thoracic aorta rings from RT and CT offspring; however, there were no significant differences in the maximal vasodilation response (CT: 99.6 ± 0.5% *v.* RT: 99.0 ± 0.7%; $n = 8$; $P = 0.238$) or sensitivity (EC_{50}) [CT: 8.1 (9.6–6.5) *v.* RT: 8.9 (9.9–7.9); $n = 8$; $P = 0.819$] to SNP between the groups (Fig. 1).

Effects of IUGR on NO content and eNOS expression in the thoracic aorta

The NO content found in the thoracic aorta homogenates from RT offspring was lower than that in those from CT offspring (CT: 426 ± 63 μM/mg of protein *v.* RT: 202 ± 21 μM/mg of protein, $n = 8$; $P < 0.05$). IUGR did not affect the protein expression of total eNOS (Fig. 2) or $eNOS^{Ser1177}$ (Fig. 3a); however, there was a significant increase in $eNOS^{Thr495}$ phosphorylation (Fig. 3b) in the thoracic aorta from RT offspring.

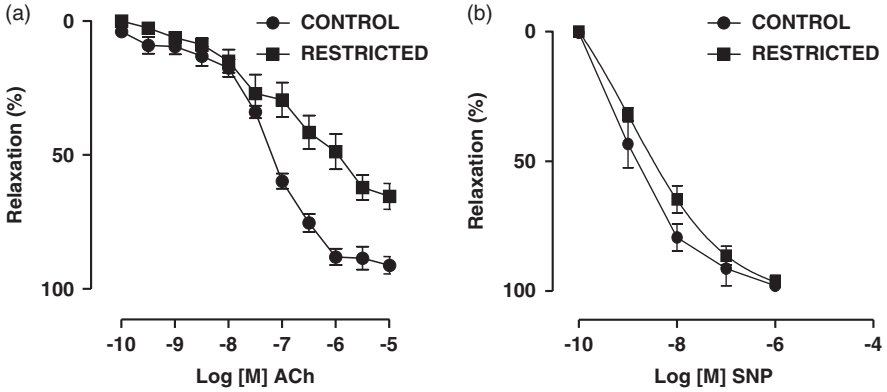

Fig. 1. Dose-dependent relaxations to (*a*) acetylcholine (ACh) and (*b*) sodium nitroprusside (SNP) in thoracic aorta rings from control and restricted offspring. Data are expressed as the percentage of noradrenaline pre-contraction.

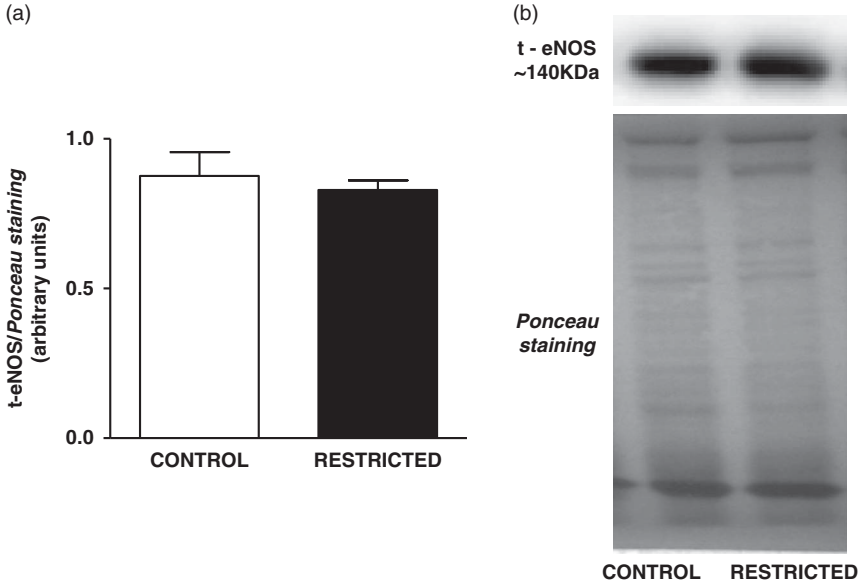

Fig. 2. Histograms show the densitometric analysis of the Western blotting for t-eNOS. Data are expressed as mean ± S.E.M. of t-eNOS/Ponceau staining (six animals/group). Student's unpaired *t*-test: $^*P < 0.05$, restricted *v.* control. Representative immunoblots of t-eNOS/Ponceau staining of the thoracic aorta from control and restricted offspring.

https://doi.org/10.1017/S2040174417000484 Published online by Cambridge University Press

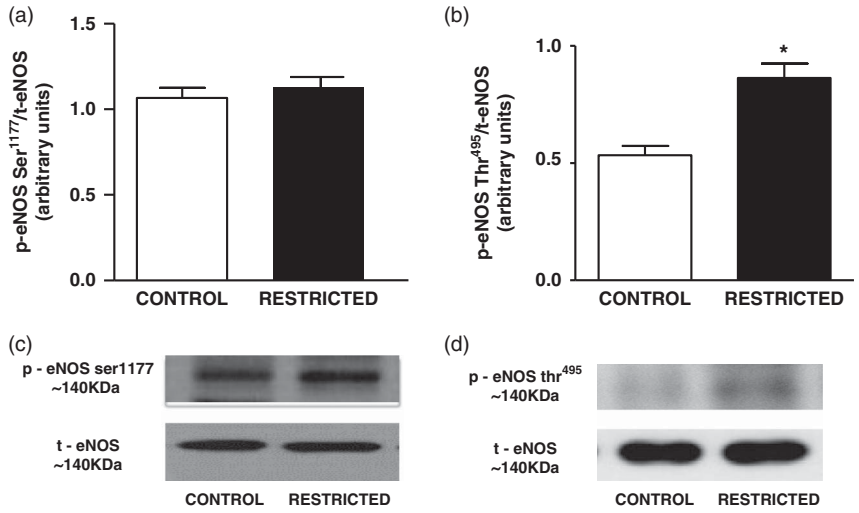

Fig. 3. Histograms show the densitometric analysis of the western blotting for (*a*) eNOS^{Ser1177} and (*b*) eNOS^{Thr495}. Data are expressed as mean ± S.E.M. of the ratio of eNOS^{Ser1177}/total eNOS and eNOS^{Thr495}/total eNOS (six animals/group). Student's unpaired *t*-test: $^{*}P < 0.05$, restricted *v.* control. Representative immunoblots of (*c*) eNOS^{Ser1177}/total eNOS and (*d*) eNOS^{Thr495}/total eNOS of the thoracic aorta from control and restricted offspring.

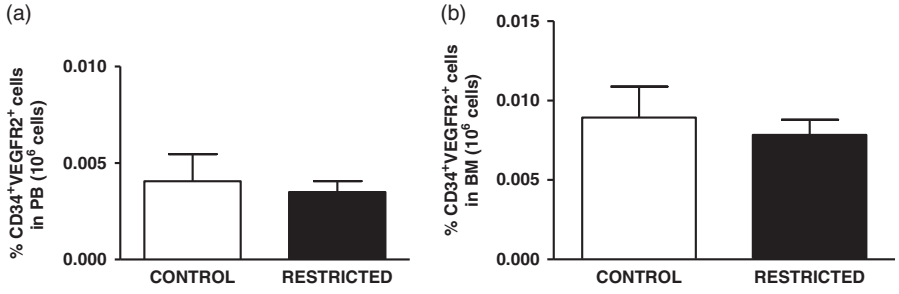

Fig. 4. Histograms show the amount of (*a*) peripheral blood-derived endothelial progenitor cells and (*b*) bone marrow-derived endothelial progenitor cells from control and restricted offspring. Data are expressed as the percentage of endothelial progenitor cells ($CD34^{+}/VEGFR2^{+}$ cells) in 10^{6} cells (7–10 animals/group). Student's unpaired *t*-test: $^{*}P < 0.05$, restricted *v.* control.

Effects of IUGR on EPC number, functional capacity and senescence in vitro

The percentage of EPCs in the PB and BM was similar between both groups (Fig. 4a and 4b). However, in comparison with the CT group, the RT group demonstrated a reduced number of CFU-EPCs in the PB and BM *in vitro* (Fig. 5a and 5b). The number of senescent cells from the BM was significantly higher in the RT group than in the CT group (Fig. 6a).

Discussion

IUGR causes deleterious changes in vascular function, contributing to increased cardiovascular risk.[1–4] The mechanisms involved have been investigated; however, little is known about the effect of IUGR on EPC properties. The present study revealed novel IUGR-induced deleterious adaptations in EPCs derived from the PB and BM. In particular, we demonstrated *in vitro* that EPC function was reduced, and the number of senescent cells from the BM was increased. In addition, IUGR did not affect the EPC number of adult male offspring.

In the present study, we observed that IUGR reduced ACh-induced vasodilation in thoracic aorta rings; however, there were no changes in SNP-induced relaxation, which was consistent with the findings of previous studies.[7,8,14] The reduced endothelium-dependent vasodilation via ACh in IUGR rats could be partly caused by lower bioavailability and/or NO production; thus, the concentration of NO was assessed. The results revealed that RT rats had lower NO levels in the thoracic aorta, which may be attributed to changes in the vascular bed, specifically increased ROS levels and reduced eNOS activity.[13,14] eNOS activity can be modulated by post-translational mechanisms including protein phosphorylation.[35] It is known that Ser1177 phosphorylation activates eNOS, whereas Thr495 phosphorylation inhibits its activity.[36–39] Therefore, these phosphorylation sites were evaluated in the aorta. Our data showed that IUGR did not affect the phosphorylation of eNOS at Ser1177; however, the phosphorylation at Thr495 was increased, suggesting that this phosphorylation site can play a role in reducing NO levels in the RT group. Although the possible mechanisms by which IUGR induces an increase in

https://doi.org/10.1017/S2040174417000484 Published online by Cambridge University Press

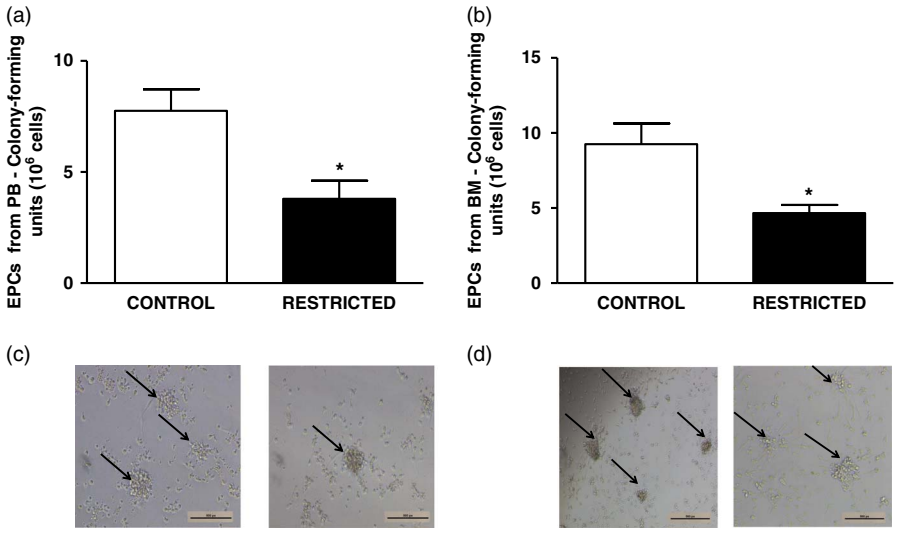

Fig. 5. Histograms show the number of colony-forming units of (*a*) peripheral blood-derived endothelial progenitor cells and (*b*) bone marrow-derived endothelial progenitor cells from control and restricted offspring. Data are expressed as mean ± S.E.M. (five animals/group). Student's unpaired *t*-test: $^*P < 0.05$, restricted *v.* control. (*c*) Black arrows show the colony-forming units of peripheral blood-derived endothelial progenitor cells and (*d*) black arrows show the colony-forming units of bone marrow-derived endothelial progenitor cells from control and restricted offspring.

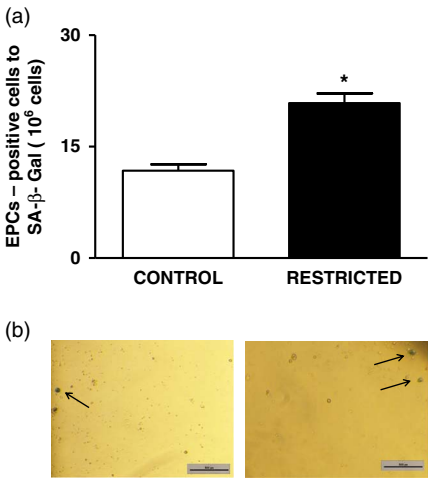

Fig. 6. (*a*) Histograms show the number of senescent endothelial progenitor cells derived from the bone marrow from control and restricted offspring. Data are expressed as mean ± S.E.M. (five animals/group). Student's unpaired *t*-test: $^*P < 0.05$, restricted *v.* control. (*b*) Black arrows show the senescent cells derived from the bone marrow from control and restricted offspring.

phosphorylation at Thr495 have not been elucidated, previous data suggest that Rho-kinase and protein kinase Cα (PCKα) could be involved. Indeed, Rho inhibition has been found to result in decrease in $eNOS^{Thr495}$ expression, while nitrite concentration was increased.[40] In addition, IUGR seems to decrease PCKα expression.[41] For this reason, it is plausible suggest that IUGR-induced NO levels could in part resulting from changes in PCKα-induced $eNOS^{Thr495}$phosphorylation.[42]

EPCs are essential for maintaining vascular healthy and endothelium repair, whereas the capacity of mature endothelial cell is limited.[15,43] Furthermore, clinical findings have emphasized the association between abnormal flow-mediated vasodilatation and impairment in EPCs number, bioavailability and/or function under pathological disorders.[28–30] Therefore, circulating EPCs has emerged as a robust marker predictor of cardiovascular diseases.[43,44] Extending these observations, experimental data have demonstrated that reduction in ACh-induced vasodilatation is followed by lower circulating EPCs amount in conditions as ageing, and hyperhomocysteinemia.[45,46] In addition, a significantly improvement in endothelial function was observed in hypertensive rats after EPCs transplantation from normotensive rats.[47] Our data evidenced that IUGR did not change the percentage of EPCs derived from PB and BM. Similar observations was reported by Ligi *et al.* They observed that IUGR has no effect on number of EPCs extracted from human umbilical cord.[27]

On the other hand, IUGR seems to play a role in functional activity of EPCs. Indeed, we showed that RT offspring had a lower CFUs-EPCs number in PB and BM, reflecting a deteriorated function *in vitro.* These results agreed with previous findings demonstrating that umbilical cord EPCs of babies, restricted *in utero*, had a significant reduction in CFUs number.[27] Data about the effects of IUGR on EPCs proprieties are scarce. However, animal models which showed endothelial dysfunction also had reduced CFU–EPCs number, or the EPCs capacity to forming colonies was completely abolished.[24,34,47,48] These previous findings support the hypothesis that EPCs dysfunction could be at least in part involved in vascular dysfunction. The mechanisms underlying negative effects in EPCs function induced by IUGR, remains to be elucidated. Nevertheless, it is known that several aspects may affect the functional capacity of EPCs.[49] Among them, accelerated senescence process of these cells seems

https://doi.org/10.1017/S2040174417000484 Published online by Cambridge University Press

to be involved.[50,51] It is important to note the EPCs viability, and hence its function is partially controlled by an adequate senescence process which, under physiological limits, play a key role as a factor for the cells survival.[52] In the present study we demonstrated that RT group showed increased number of senescent EPCs derived from BM, as evidenced by the positive staining by SA-β-Gal. It should be considered that senescent cells remain viable, but considerable changes on its morphology and function are observed.[53–55] The high senescent cells number found in RT rats may have contributed partially to reduce EPCs function *in vitro*. Cells can become senescent promptly, independently of rate of cells division.[56] Factors as high ROS levels and lack of nutrients can induce senescence, which is designated as stress-induced premature senescence.[57,58] Accelerated senescence in EPCs has been attributed in part to increased oxidative stress, due to NADPH activation, that induces upregulation in p38 mitogen activated protein kinase phosphorylation.[59,60] In summary, our data provides evidence that IUGR rats show deleterious changes in EPCs, as reduction in EPCs function and accelerated senescence *in vitro*. These findings may collaborate in part to clarify the possible mechanisms involved in endothelial dysfunction induced by fetal programming.

Acknowledgements

The authors thank Dr Maria Aparecida Dalboni from Federal University of São Paulo for her excellent support in flow cytometer analysis.

Financial Support

This research was supported by Grant from the *FAPESP* (*Fundação de Amparo à Pesquisa do Estado de São Paulo*, Brazil) (Project Number: 2013/03139-0). Vanessa Oliveira is supported by a fellowship from the *FAPESP* (2013/00311-6).

Conflicts of Interest

None.

Supplementary material

To view supplementary material for this article, please visit https://doi.org/10.1017/S2040174417000484

References

1. Faienza MF, Brunetti G, Delvecchio M, *et al*. Vascular function and myocardial performance indices in children born small for gestational age. *Circ J*. 2016; 4, 958–963.
2. Franco MC, Higa EM, D'Almeida V, *et al*. Homocysteine and nitric oxide are related to blood pressure and vascular function in small-for-gestational-age children. *Hypertension*. 2007; 2, 396–402.
3. Martin H, Hu J, Gennser G, *et al*. Impaired endothelial function and increased carotid stiffness in 9-year-old children with low birth weight. *Circulation*. 2000; 102, 2739–2744.
4. Herrera EA, Cifuentes-Zuniga F, Figueroa E, *et al*. N-acetyl cysteine, a glutathione precursor, reverts vascular dysfunction and endothelial epigenetic programming in intrauterine growth restricted guinea pigs. *J Physiol*. 2016; 595, 1077–1092.
5. Holemans K, Gerber R, Meurrens K, *et al*. Maternal food restriction in the second half of pregnancy affects vascular function but not blood pressure of rat female offspring. *Br J Nutr*. 1999; 81, 73–79.
6. Renshall LJ, Dilworth MR, Greenwood SL, *et al*. In vitro assessment of mouse fetal abdominal aortic vascular function. *Am J Physiol Regul Integr Comp Physiol*. 2014; R746–R754.
7. Torrens C, Hanson MA, Gluckman PD, *et al*. Maternal undernutrition leads to endothelial dysfunction in adult male rat offspring independent of postnatal diet. *Br J Nutr*. 2009; 101, 27–33.
8. Franco M, Akamine EH, Dimarco GS, *et al*. NADPH oxidase and enhanced superoxide generation in the intrauterine undernourished rats: involvement of the renin-angiotensin system. *Cardiovasc Res*. 2003; 59, 767–775.
9. Itani N, Skeffington KL, Beck C, *et al*. Melatonin rescues cardiovascular dysfunction during hypoxic development in the chick embryo. *J Pineal Res*. 2016; 60, 16–26.
10. Tarry-Adkins JL, Martin-Gronert MS, Chen JH, *et al*. Maternal diet influences DNA damage, aortic telomere length, oxidative stress, and antioxidant defense capacity in rats. *FASEB J*. 2008; 22, 2037–2044.
11. Khorram O, Chuang TD, Pearce WJ. Long-term effects of maternal undernutrition on offspring carotid artery remodeling: role of miR-29c. *J Dev Orig Health Dis*. 2015; 4, 342–349.
12. Kane AD, Herrera EA, Camm EJ, *et al*. Vitamin C prevents intrauterine programming of in vivo cardiovascular dysfunction in the rat. *Circ J*. 2013; 77, 2604–2611.
13. Oliveira V, Akamine EH, Carvalho MHC, *et al*. Influence of aerobic training on the reduced vasoconstriction to angiotensin II in rats exposed to intrauterine growth restriction: possible role of oxidative stress and AT2 receptor of angiotensin II. *PLoS One*. 2014; 11, e113035.
14. Franco Mdo C, Arruda RM, Dantas AP, *et al*. Intrauterine undernutrition: expression and activity of the endothelial nitric oxide synthase in male and female adult offspring. *Cardiovasc Res*. 2002; 56, 145–153.
15. Asahara T, Murohara T, Sullivan A, *et al*. Isolation of putative progenitor endothelial cells for angiogenesis. *Science*. 1997; 275, 964–967.
16. Shi Q, Rafii S, Wu MH, *et al*. Evidence for circulating bone marrow-derived endothelial cells. *Blood*. 1998; 92, 362–367.
17. Zhang M, Malik AB, Rehman J. Endothelial progenitor cells and vascular repair. *J Curr Opin Hematol*. 2014; 3, 224–228.
18. Van Zonneveld AJ, Rabelink TJ. Endothelial progenitor cells: biology and therapeutic potential in hypertension. *Curr Opin Nephrol Hypertens*. 2006; 15, 167–172.
19. Urbich C, Dimmeler S. Endothelial progenitor cells: characterization and role in vascular biology. *Circ Res*. 2004; 95, 343–353.
20. Jansen F, Yang X, Hoelscher M, *et al*. Endothelial microparticle-mediated transfer of microRNA-126 promotes vascular endothelial cell repair via SPRED1 and is abrogated in glucose-damaged endothelial microparticles. *Circulation*. 2013; 128, 2026–2038.
21. Hill JM, Zalos G, Halcox JP, *et al*. Circulating endothelial progenitor cells, vascular function, and cardiovascular risk. *N Engl J Med*. 2003; 348, 593–600.

22. Vasa M, Fichtlscherer S, Aicher A, *et al*. Number and migratory activity of circulating endothelial progenitor cells inversely correlate with risk factors for coronary artery disease. *Circ Res*. 2001; 89, E1–E7.
23. Imanish T, Kobayashi K, Hano T, *et al*. Effect of estrogen on differentiation and senescence in endothelial progenitor cells derived from bone marrow in spontaneously hypertensive rats. *Hypert Res*. 2005; 28, 763–772.
24. Imanish T, Moriwak C, Hano T, *et al*. Endothelial progenitor cell senescence is accelerated in both experimental hypertensive rats and patients with essential hypertension. *J Hypert*. 2005; 23, 1831–1837.
25. Schmidt-Lucke C, Rössig L, Fichtlscherer S, *et al*. Reduced number of circulating endothelial progenitor cells predicts future cardiovascular events: proof of concept for the clinical importance of endogenous vascular repair. *Circulation*. 2005; 111, 2981–2987.
26. Oikonomou E, Siasos G, Zaromitidou M, *et al*. Atorvastatin treatment improves endothelial function through endothelial progenitor cells mobilization in ischemic heart failure patients. *Atherosclerosis*. 2015; 2, 159–164.
27. Ligi I, Simoncini S, Tellier E, *et al*. A switch toward angiostatic gene expression impairs the angiogenic properties of endothelial progenitor cells in low birth weight preterm infants. *Blood*. 2011; 118, 1699–1709.
28. Miura M, Numaguchi Y, Ishii M, *et al*. Differentiation capacity of endothelial progenitor cells correlates with endothelial function in healthy young men. *Circ J*. 2009; 73, 1324–1329.
29. Sibal L, Aldibbiat A, Agarwal SC, *et al*. Circulating endothelial progenitor cells, endothelial function, carotid intima-media thickness and circulating markers of endothelial dysfunction in people with type 1 diabetes without macrovascular disease or microalbuminuria. *Diabetologia*. 2009; 52, 1464–1473.
30. Palombo C, Kozakova M, Morizzo C, *et al*. Circulating endothelial progenitor cells and large artery structure and function in young subjects with uncomplicated type 1 diabetes. *Cardiovasc Diabetol*. 2011; 10, 88.
31. Hampl V, Walters CL, Archer SL. Determination of nitric oxide by the chemiluminescence reaction with ozone. In *Methods in Nitric Oxide Research* (eds. Feelisch M, Stamler JS), 1996; pp. 310–318. John Wiley & Sons: Chichester.
32. Romero-Calvo I, Ocón B, Martínez-Moya P, *et al*. Reversible Ponceau staining as a loading control alternative to actin in Western blots. *Anal Biochem*. 2010; 401, 318–320.
33. Aldridge GM, Podrebarac DM, Greenough WT, *et al*. The use of total protein stains as loading controls: an alternative to high-abundance single-protein controls in semi-quantitative immunoblotting. *J Neurosci Methods*. 2008; 172, 250–254.
34. Fernandes T, Nakamuta JS, Magalhães FC, *et al*. Exercise training restores the endothelial progenitor cells number and function in hypertension: implications for angiogenesis. *J Hypertens*. 2012; 30, 2133–2143.
35. Qian J, Fulton D. Post-translational regulation of endothelial nitric oxide synthase in vascular endothelium. *Front Physiol*. 2013; 4, 347.
36. Church JE, Fulton D. Differences in eNOS activity because of subcellular localization are dictated by phosphorylation state rather than the local calcium environment. *J Biol Chem*. 2006; 281, 1477–1488.
37. Michell BJ, Chen Z, Tiganis T, *et al*. Coordinated control of endothelial nitric-oxide synthase phosphorylation by protein kinase C and the cAMP-dependent protein kinase. *J Biol Chem*. 2001; 276, 17625–17628.
38. Harris MB, Ju H, Venema VJ, *et al*. Reciprocal phosphorylation and regulation of endothelial nitric-oxide synthase in response to bradykinin stimulation. . *J Biol Chem*. 2001; 276, 16587–16591.
39. Fleming I, Fisslthaler B, Dimmeler S, *et al*. Phosphorylation of Thr(495) regulates Ca(2 +)/calmodulin-dependent endothelial nitric oxide synthase activity. *Circ Res*. 2001; 88, E68–E75.
40. Watts VL, Motley ED. Role of protease-activated receptor-1 in endothelial nitric oxide synthase-Thr495 phosphorylation. *Exp Biol Med (Maywood)*. 2009; 234, 132–139.
41. Sugden MC, Langdown ML. Possible involvement of PKC isoforms in signalling placental apoptosis in intrauterine growth retardation. *Mol Cell Endocrinol*. 2001; 185, 119–126.
42. Li P, Zhang L, Zhang M, *et al*. Uric acid enhances PKC-dependent eNOS phosphorylation and mediates cellular ER stress: a mechanism for uric acid-induced endothelial dysfunction. *Int J Mol Med*. 2016; 37, 989–997.
43. Werner N, Koriol S, Schiegl T, *et al*. Circulating endothelial progenitor cells and cardiovascular outcomes. *N Engl J Med*. 2005; 353, 999–1007.
44. Schmidt-Lucke C, Rossig L, Fichtlscherer S, *et al*. Reduced number of circulating endothelial progenitor cells predicts future cardiovascular events: proof of concept for the clinical importance of endogenous vascular repair. *Circulation*. 2005; 111, 2981–2987.
45. Sun Q, Dong Y, Wang HJ, *et al*. Anti-peroxynitrite treatment ameliorates vasorelaxation of resistance arteries in aging rats: involvement with protection of circulating endothelial progenitor cells. *J Cardiovasc Pharmacol*. 2016 [Epub ahead of print].
46. Dong Y, Sun Q, Liu T, *et al*. Nitrative stress participates in endothelial progenitor cell injury in hyperhomocysteinemia. *PLoS One*. 2016; 11, e0158672.
47. Yu H, Shao H, Yan J, *et al*. Bone marrow transplantation improves endothelial function in hypertensive Dahl salt-sensitive rats. *J Am Soc Hypertens*. 2012; 5, 331–337.
48. Yoshida Y, Fukuda N, Maeshima A, *et al*. Treatment with valsartan stimulates endothelial progenitor cells and renal label-retaining cells in hypertensive rats. *J Hypertens*. 2011; 29, 91–101.
49. Imanishi T, Tsujioka H, Akasaka T. Endothelial progenitor cells dysfunction and senescence: contribution to oxidative stress. *Curr Cardiol Rev*. 2008; 4, 275–286.
50. Vassallo PF, Simoncini S, Ligi I, *et al*. Accelerated senescence of cord blood endothelial progenitor cells in premature neonates is driven by SIRT1 decreased expression. *Blood*. 2014; 13, 2116–2126.
51. Liu B, Li T, Peng JJ, *et al*. Non-muscle myosin light chain promotes endothelial progenitor cells senescence and dysfunction in pulmonary hypertensive rats through up-regulation of NADPH oxidase. *Eur J Pharmacol*. 2016; 775, 67–77.
52. Ben-Porath I, Weinberg RA. When cells get stressed: an integrative view of cellular senescence. *J Clin Invest*. 2004; 113, 8–13.
53. Wright WE, Shay JW. Histological claims and current interpretations of replicative aging. . *Nat Biotechnol*. 2002; 20, 682–688.
54. Sherr CJ, De Pinho RA. Cellular senescence: mitotic clock or culture shock? *Cell*. 2000; 102, 407–410.
55. Sitte N, Merker K, Von Zglinicki T, *et al*. Protein oxidation and degradation during cellular senescence of human BJ

fibroblasts: part I – effects of proliferative senescence. *FASEB J*. 2000; 15, 2495–2502.
56. Robles SJ, Adami GR. Agents that cause DNA double strand breaks lead to p16INK4a enrichment and the premature senescence of normal fibroblasts. *Oncogene*. 1998; 16, 1113–1123.
57. Kaneko T, Tahara S, Taguchi T, Kondo H. Accumulation of oxidative DNA damage, 8-oxo-2'-deoxyguanoside, and change of repair systems during in vitro cellular aging of cultured human skin fibroblasts. *Mutat Res*. 2001; 487, 19–30.
58. Chen Q, Ames BN. Senescence-like growth arrest induced by hydrogen peroxide in human diploid fibroblast F65 cells. *Proc Natl Acad Sci USA*. 1994; 91, 4130–4134.
59. Kuki S, Imanishi T, Kobayashi K, *et al*. Hyperglycemia accelerated endothelial progenitor cell senescence via an activation of p38 mitogen-activated protein kinase. *Circ J*. 2006; 70, 1076–1081.
60. Seeger FH, Haendeler J, Walter DH, *et al*. p38 mitogen-activated protein kinase downregulates endothelial progenitor cells. *Circulation*. 2005; 111, 1184–1191.